Progressive vascular changes in a transgenic mouse model of squamous cell carcinoma

Jason A. Hoffman,[1,3,4] Enrico Giraudo,[2,4] Mallika Singh,[2,4,6] Lianglin Zhang,[1] Masahiro Inoue,[2,5,7] Kimmo Porkka,[1,5] Douglas Hanahan,[2,*] and Erkki Ruoslahti[1,*]

[1]Cancer Research Center, The Burnham Institute, 10901 North Torrey Pines Road, La Jolla, California 92037
[2]Department of Biochemistry and Biophysics and the Diabetes and Comprehensive Cancer Centers, University of California, San Francisco, 513 Parnassus Avenue, San Francisco, California 94143
[3]Program in Molecular Pathology, The Burnham Institute and Department of Pathology, University of California, San Diego, School of Medicine, 9500 Gilman Drive, La Jolla, California 92093
[4]These authors contributed equally to this work.
[5]These authors contributed equally to this work.
[6]Present address: Exelixis Inc., 170 Harbor Way, South San Francisco, California 94083.
[7]Present address: Osaka Medical Center for Cancer and Cardiovascular Diseases, Department of Biochemistry, 1-3-3 Nakamichi, Higashinari-ku, Osaka 537-8511, Japan.
*Correspondence: ruoslahti@burnham.org (E.R.); dh@biochem.ucsf.edu (D.H.)

Summary

Phage display was used to identify homing peptides for blood vessels in a mouse model of HPV16-induced epidermal carcinogenesis. One peptide, CSRPRRSEC, recognized the neovasculature in dysplastic skin but not in carcinomas. Two other peptides, with the sequences CGKRK and CDTRL, preferentially homed to neovasculature in tumors and, to a lesser extent, premalignant dysplasias. The peptides did not home to vessels in normal skin, other normal organs, or the stages in pancreatic islet carcinogenesis in another mouse model. The CGKRK peptide may recognize heparan sulfates in tumor vessels. The dysplasia-homing peptide is identical to a loop in kallikrein-9 and may bind a kallikrein inhibitor or substrate. Thus, characteristics of the angiogenic vasculature distinguish premalignant and malignant stages of skin tumorigenesis.

Introduction

Tumorigenesis is a multistage process that involves multiple cell types (Hanahan and Weinberg, 2000). One contributory cell type is the tumor endothelia that line blood and lymphatic vessels (Ruoslahti, 2002). These cells form a tumor's prerequisite blood vascular system during angiogenesis and also line the two routes used by tumor cells to metastasize. Angiogenesis is already apparent in the premalignant lesions of human tumors and transgenic mouse tumor models (Hanahan and Folkman, 1996). The new blood vessels in neoplasias are often structurally and functionally abnormal (Carmeliet and Jain, 2000; Pasqualini et al., 2002) and may be at different stages of normal maturation during physiological angiogenesis (Gee et al., 2003).

The K14-HPV16 transgenic tumor model expresses human papillomavirus type 16 (HPV16) oncogenes under control of the keratin-14 (K14) promoter. These mice express the HPV16 E6 and E7 oncogenes in the basal cells of their squamous epithelia (Arbeit et al., 1994); in the FVB/n strain background, they spontaneously develop epidermal squamous cell cancers (SCC) in a multistage fashion (Coussens et al., 1996). Their skin appears normal at birth but becomes hyperplastic within the first month, and focal dysplasias develop between 3 and 6 months of age. These focal dysplasias are angiogenic and by one year, these lesions develop into invasive SCCs in about half of the mice. Progression is accompanied by the upregulation of pro-angiogenic factors such as VEGF (Smith-McCune et al., 1997) and bFGF (Arbeit et al., 1996), and the model has called attention to the involvement of proteases from inflammatory mast cells (Coussens et al., 1999) and other bone marrow-derived cells (neutrophils and macrophages) in angiogenesis and tumor progression (Coussens et al., 2000).

In vivo phage display has revealed peptides that target tumor endothelial cells (Arap et al., 1998) or tumor pericytes (Burg et al., 1999). A combination of in vivo and ex vivo phage display (Hoffman et al., 2004) has further expanded the discriminatory

SIGNIFICANCE

Antiangiogenic therapies for the treatment of cancers have the promise of high efficacy and low toxicity. The complex responses to antiangiogenic therapy likely reflect our incomplete understanding of the alterations that blood vessels experience during tumor development and of how tumor types might molecularly differ in their neovascular parameters. We have discovered peptides that differentially recognize blood vessels at distinctive stages of tumor progression in squamous carcinogenesis, predicting neovascular heterogeneity between premalignant and malignant stages. These peptides present a means to define molecular determinants relevant to the varying responses to antiangiogenic therapies and could serve as vehicles for targeting imaging agents and therapeutics to tumor blood vessels in a tumor type- and stage-specific manner.

power of that methodology, yielding peptides that recognize a shared cell surface specificity among tumor blood vessels, tumor cells, and bone marrow cells (Porkka et al., 2002) or tumor lymphatic endothelium and tumor cells (Laakkonen et al., 2002).

The goal of the present study was to evaluate the molecular changes that occur in blood vessels as they develop from angiogenic vessels in dysplasias to tumor blood vessels. Our aim to compare the vasculature in premalignant and malignant lesions was motivated in part by studies in another mouse model (RIP-Tag) demonstrating that the efficacy of certain angiogenesis inhibitors varied as a function of stage: several inhibitors were most effective against angiogenic dysplasias (progenitors), whereas other compounds were more effective against later stages (Bergers et al., 1999, 2003). Thus the premalignant (and nascent tumor) vasculature may have distinctive qualities as compared to those of the mature tumor vasculature. Indeed, this study supports that proposition. Herein we isolate and describe three peptides in depth that home via the circulation to the neovasculature. One recognizes a binding moiety that is preferentially expressed in skin dysplasias, but is low or absent in tumors and in normal vasculature. Two other peptides homed to tumors and to a lesser extent to dysplastic skin vasculature of tumor-bearing mice. All three peptides variably home to other tumor types growing in or under the skin, but none recognize the vasculature of angiogenic dysplasias or tumors in the RIP-Tag transgenic mouse model of pancreatic islet carcinoma. These results, and those reported in the accompanying paper (Joyce et al., 2003 [this issue of *Cancer Cell*]) that similarly profiles the vasculature in the RIP-Tag model, show that the vessels of premalignant and fully malignant lesions are distinguishable and that different tumors express distinct repertoires of molecular markers in their vasculature.

Results

Selecting phage that home to dysplastic skin

We used a previously described library of T7 bacteriophage that display on their surface 9-mer cyclic peptides with seven degenerate positions (CX_7C) (Laakkonen et al., 2002). To isolate peptides specific for dysplasia, we performed two rounds of selection ex vivo and one round in vivo. For the ex vivo rounds, we incubated the phage with dispersed cells from dysplastic skin removed from the ears and chest of K14-HPV16 mice at 4–6 months of age. The biopsied lesions typically included a focal region of epidermal dysplasia flanked by adjacent hyperplastic epidermis, along with the underlying reactive stromal elements and angiogenic endothelium in the aberrant dermis. A portion of each tissue biopsy used for ex vivo or subsequent in vivo rounds of phage selection was fixed in formalin and, after conventional processing, examined histologically to assess the neoplastic grade. H&E-stained paraffin sections confirmed that the areas of skin used in these selection steps were largely comprised of focal dysplasias (data not shown). The sequential ex vivo selections on cell suspensions of dysplastic skin resulted in a 160-fold enrichment of phage relative to similar treatment with nonrecombinant phage that lack displayed peptides (Figure 1A, left); a greater than 10,000-fold enrichment resulted from the subsequent in vivo round (Figure 1A, right). Selection in vivo also produced a minor enrichment of phage that homed to the control tissues: brain, kidney, and hyperplastic skin. We performed DNA sequence analysis of 48 clones isolated in the second ex vivo round and 48 clones from the subsequent in vivo round (data not shown) to identify the CX_7C peptides that had been selected. Nine peptides that appeared most frequently amongst the 96 phage display clones analyzed were chosen for further examination.

To test the homing specificity of these peptide sequences, we intravenously injected purified phage displaying a particular sequence into K14-HPV16 mice bearing protuberant tumors or alternatively presenting with multifocal dysplasias but no tumors. Both neoplastic tissues and normal control organs were collected and assayed for accumulation of phage. Phage displaying the peptide CRAKSKVAC, which appeared with the highest frequency in both the ex vivo (5 times) and in vivo sequence pools (15 times), were 1500-fold enriched in dysplastic skin relative to nonrecombinant control phage (data not shown). However, phage displaying this peptide accumulated with similar frequencies in skin, kidney, and brain (data not shown), indicating that the CRAKSKVAC sequence homes to an abundant signal in each of these organs and is not specific to the skin lesions of interest here. Six other of the dysplasia-selected clones also differentiated poorly between the control tissues and dysplastic skin in these tests. Altogether, 7 of the 9 dysplasia phage clones appeared to be responsible for the overall enrichment of the pool in the control tissues observed in the final in vivo round (Figure 1A, right) and were not considered suitable candidates for further study. The insert sequences in the two remaining phage clones were found to be highly selective for dysplastic skin and did not appreciably home to normal organs. One of these peptides, CNRRTKAGC, is closely related to a previously described peptide that homes to tumor lymphatic vessels (Laakkonen et al., 2002) and was not further analyzed here. The second dysplasia-homing peptide, CSRPRRSEC, was novel in our experience; it appeared three times amongst the 48 phage sequenced from the in vivo round, along with two variants: CSRPRRSVC and CSRPRRSWC that appeared one time each. Phage displaying the CSRPRRSEC peptide were enriched ~350-fold in dysplastic skin and did not significantly accumulate in the control tissues (Figure 1C). When injected into a K14-HPV16 mouse bearing an ear tumor as well as multifocal skin dysplasias, the CSRPRRSEC phage effectively homed to dysplastic chest skin and dysplastic ear skin, but showed little homing to the tumor (Figure 1C). The peptide-bearing phage did not home to the normal skin of FVB/n mice in vivo (Figure 1C) and did not bind in ex vivo experiments to the hyperplastic skin of 1- to 2-month-old K14-HPV16 mice (data not shown). These results indicate that the CSRPRRSEC peptide selectively homes to dysplastic lesions; we infer that the CSRPRRSEC peptide binds to a molecule (a "receptor") that is present in skin dysplasias, but is essentially absent or inaccessible via the circulation in normal skin or in SCCs.

Tumor-specific homing phage

To isolate phage that home to SCCs in K14-HPV16 mice, we performed two rounds of ex vivo and two rounds of in vivo selections on tumors histologically confirmed as squamous cell carcinoma grades II–IV (Coussens et al., 1996). The enrichment rose from 6-fold in the second ex vivo round to greater than 70-fold in the second in vivo round (the fourth sequential round overall) (Figure 1B). Fifteen phage clones were selected for further analysis based on their frequent appearance amongst 192 sequenced clones (48 from ex vivo round 2, 48 from in vivo round

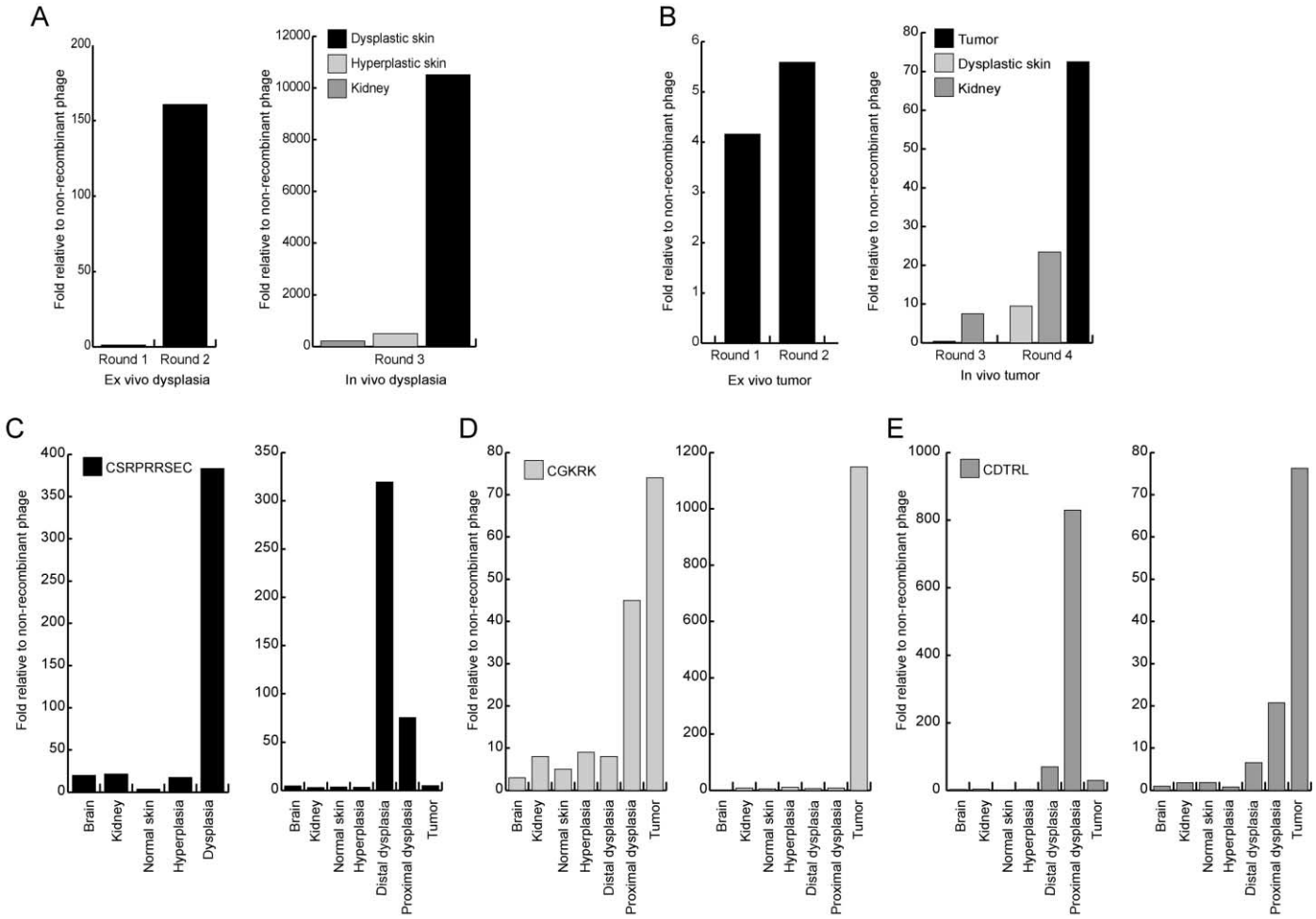

Figure 1. Phage-displayed peptides home to dysplastic skin lesions and tumors

Ex vivo and in vivo selections of phage for binding and homing to dysplastic skin lesions (**A**) or tumors (**B**).

C: In vivo homing of the CSRPRRSEC from the dysplastic skin screen to dysplastic skin lesions of a 4- to 6-month-old K14-HPV16 mouse (left) and to dysplastic skin lesions and tumor of a 9- to 12-month-old K14-HPV16 mouse (right).

In vivo homing of CGKRK (**D**) and CDTRL (**E**) peptides from tumor screening to tumors and other tissues in K14-HPV16 mice. Results from two different tumor-bearing mice are shown for each peptide. The normal skin values shown in **C–E** are from parallel experiments in wild-type FVB/n mice.

1, and 96 from in vivo round 2) and their increased appearance in the in vivo rounds. Of these, four clones with amino acid sequences CGKRK, CGTKRKC, CDTAVVEGL, and CDTRL bound to a K14-HPV16 tumor-derived cell suspension ex vivo. Phage-displayed CDTAVVEGL also homed in vivo 340-fold to tumors (data not shown), but we had difficulties with the CDTAVVEGL peptide in the subsequent steps, so we could not work further with the peptide. The remaining three phage-displayed peptides, CDTRL and the related CGKRK and CGTKRKC, were analyzed in depth.

When intravenously injected into tumor-bearing K14-HPV16 mice, the CGKRK phage showed a marked preference for the tumor, with an efficiency that varied from 80- to 1,000-fold in two experiments. Some homing to dysplastic lesions was observed in one of two experiments that showed an 80× enrichment in the tumor (Figure 1D). Normal and hyperplastic skin and various control organs also accumulated CGKRK phage but at very low levels (Figure 1D and data not shown). Similar analysis of the CDTRL phage revealed a variable preference for SCCs and dysplastic lesions; in one experiment, the phage accumulated more effectively in dysplastic lesions than in a tumor, whereas the reverse was true in another experiment (Figure 1E). This phage showed little affinity for hyperplastic skin and no significant homing to normal skin from FVB/n mice (Figure 1E). Thus, phage displaying this peptide were variably selective for both dysplasias and squamous tumors of the epidermis, indicative of lesional heterogeneity in the moiety to which it binds. The squamous cancers that arise in the HPV16 model are heterogeneous, showing variations that can be scored by classical grading schemes for squamous tumors (Grades I–IV), as reported in Coussens et al. (1996); in addition, distinctive sebaceous cell carcinomas arise. Furthermore, the angiogenic dysplasias undergo morphological progression as the lesions progress from hyperplasia to low to high grade dysplasia, and thus it would not be surprising if there was variability in expression of certain binding moieties as a function of both premaligant and malignant progression.

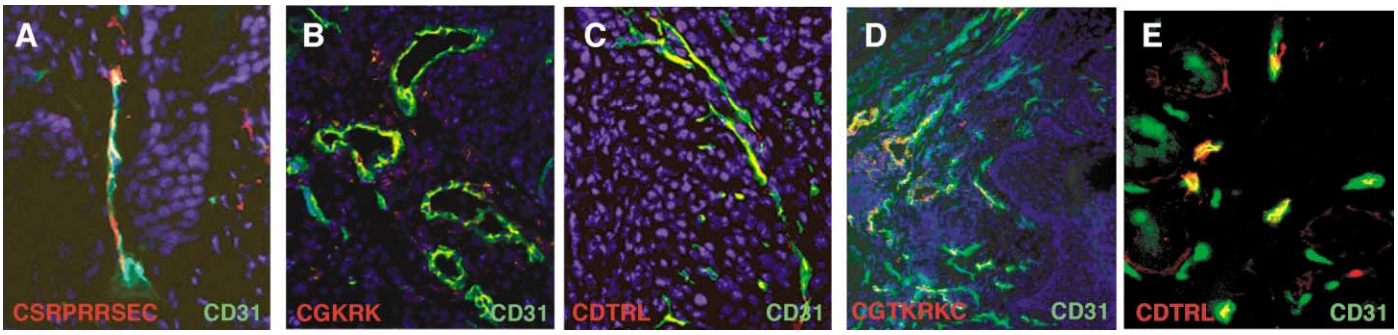

Figure 2. Vascular localization of homing phage

K14-HPV16 mice with dysplastic skin lesions or tumors were intravenously injected with individual homing phage, the mice were sacrificed 10 min later, and the phage were detected in tissue sections with rabbit anti-T7 phage (red; Alexa594). Blood vessels were stained with rat anti-mouse CD31 (green; Alexa488). **A:** CSRPRRSEC-displaying phage colocalizes with CD31 in the dysplastic skin lesions of 4- to 6-month-old dysplastic mice. **B–E:** The tumor-homing KRK-containing phage (**B** and **D**) and CDTRL (**C** and **E**) phage home to CD31-positive vessels in skin tumor (**B** and **C**) and dysplasia (**D** and **E**). Original magnifications: ×400 (**A** and **E**), ×200 (**B**–**D**).

Intra-tissue localization of homing peptides

To begin characterizing the nature of the selectivity of the dysplasia- and tumor-homing peptides for these neoplastic lesions, we sought to visualize their localization using histological procedures. K14-HPV16 mice were intravenously injected with cloned phage displaying a particular peptide or with the chemically synthesized, fluorescein-labeled peptide. We first evaluated the phage, intravenously injecting 4- to 6-month-old dysplasia-bearing mice with the dysplasia-homing phage, presenting CSRPRRSEC. In parallel, a set of 9- to 12-month-old tumor-bearing mice were infused with one or the other of the tumor-homing phage, CGTKRKC, CGKRK, or CDTRL. Various tissues were collected from each mouse and subjected to double label immunohistochemical staining, with an anti-T7 antibody to detect phage and with an anti-CD31 antibody that marks the endothelial cells of the vasculature. In each case, the phage colocalized with CD31-positive endothelial cells in the target tissue: CSRPRRSEC in dysplastic skin (Figure 2A) and CGKRK (Figure 2B) and CDTRL (Figure 2C) in tumors. The CGTKRKC phage was also detected to a lesser extent in the dysplastic skin of a tumor-bearing mouse (Figure 2D), and the positive vessels were often around what appeared to be concentric, nested clusters of keratinocytes, while the CDTRL phage was observed in large, dilated vessels throughout the dysplastic and hyperplastic skin (Figure 2E). Hematoxylin and eosin staining of serial sections adjacent to those used to visualize phage localization facilitated identification of the tissue structure to which the peptides were binding (see Supplemental Figure S1 at http://www.cancercell.org/cgi/content/full/4/5/383/DC1).

To further evaluate the homing specificity of the displayed peptides, we similarly analyzed pure peptides outside the context of the phage particles. We injected both younger dysplasia-bearing and older tumor-bearing K14-HPV16 mice with each of the fluorescein-labeled peptides. After 10 min, both normal and neoplastic tissues were collected; tissue sections were prepared and stained with antibodies to both CD31 and a second endothelial marker, the cell-surface antigen MECA32. Similar results were obtained with the two antibodies; the data for MECA32 are shown. Localizations of the intravenously infused peptides and the antibody were visualized by two-color fluorescence microscopy. The fluorescein-labeled peptides colocalized with MECA32 in their target neoplastic tissue after an intravenous injection and were not detected in tissues where the corresponding phage did not home. Fluorescein-CSRPRRSEC colocalized with MECA32 in dysplastic skin vasculature from both non-tumor-bearing (Figure 3A) and tumor-bearing mice (Figure 3D, inset); notably, the peptide was not detected within the squamous tumor in the latter (Figure 3D), confirming its selectivity for the premalignant dysplastic vasculature. In contrast, the fluorescein-labeled CGKRK (Figure 3B) and CDTRL (Figure 3C) peptides were not detected in the dysplastic skin of younger non-tumor-bearing mice but were primarily detected in tumor vasculature (Figures 3E and 3F) and at lower levels in the dysplastic skin of these tumor-bearing mice (data not shown). Again, H&E staining of serial sections guided morphological evaluation of the binding patterns (see Supplemental Figure S2 on *Cancer Cell* website). A fluorescein-conjugated control peptide (NSSSVDK) did not home to any tissue. Taken together with the immunolocalization analyses of phage homing, the peptide localization data indicate that CGKRK and CDTRL home specifically to blood vessels in SCCs and in the dysplastic foci of tumor-bearing mice, but not to the vasculature of earlier stage dysplasias in non-tumor-bearing mice.

Tumor type specificity of peptide homing

The peptides identified by their binding to endothelial cells in skin dysplasias or skin tumors could in principle be selective for neoplasias in this tissue, neoplasias of this cell type, or neoplasias induced by these oncogenes or be general to neoplasias in various tissues and of various cell types and oncogenic transformations. To begin investigating this question, we asked whether the K14-HPV16 SCC-homing peptides, CGKRK and CDTRL, would home to the endothelium in tumors that are of different tissue origins and/or are resident in different anatomical locations. To this end, we examined three subcutaneous tumors arising from inoculated tumor cell lines, two other transgenic mouse models of organ-specific tumorigenesis, and subcutaneously transplanted matrigel pellets embedded with VEGF and bFGF. Each was assessed for selective binding to the neovasculature of intravenously injected fluorescein-labeled peptides (Figure 4; Supplemental Figure S3 on *Cancer Cell* website). We observed distinctive homing specificities for the two peptides

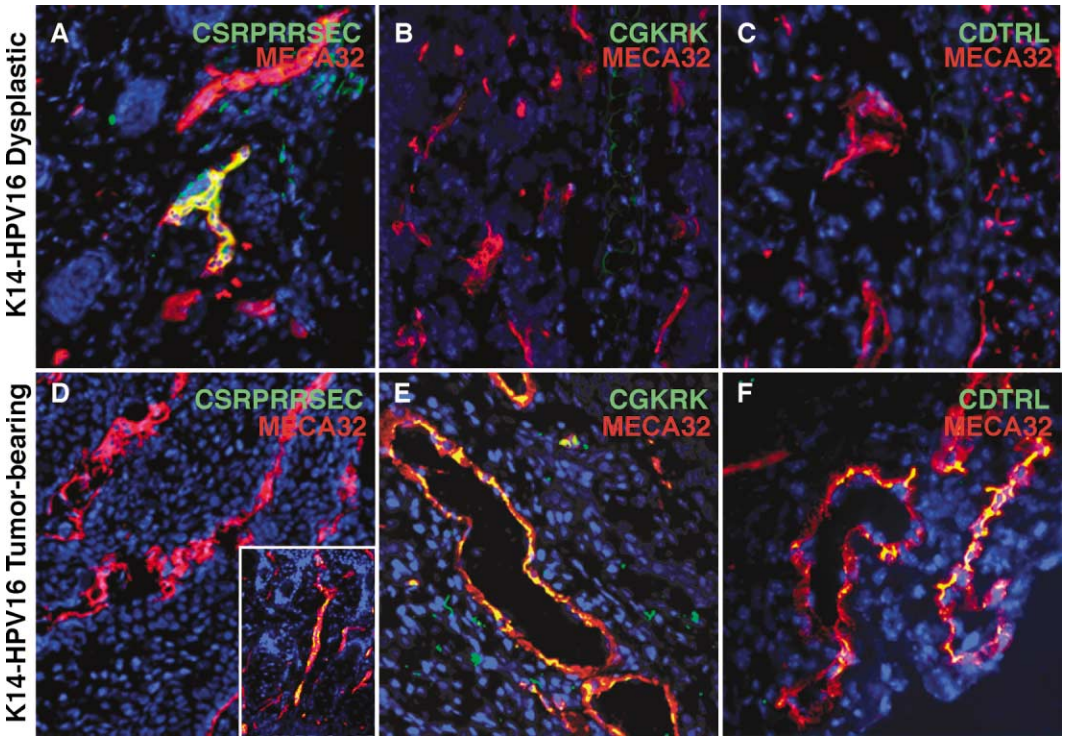

Figure 3. Fluorescein-labeled peptides colocalize with a vascular marker

Fluorescein-labeled peptides were intravenously injected into mice with dysplastic skin lesions or tumors, the mice were sacrificed 10 min later, and the peptide localization was examined in tissue sections. Fluorescein-CSRPRRSEC colocalizes with MECA32 in the vasculature of dysplastic skin (**A**) but not in tumor tissue (**D**). This peptide continues to recognize the vasculature of dysplastic skin in tumor-bearing mice (**D** inset). This peptide does not recognize premalignant lesions (angiogenic islets) in RIP1-Tag2 mice. Fluorescein-labeled CGKRK and CDTRL peptides were not detected in dysplastic skin from 4- to 6-month-old mice (**B** and **C**), but colocalized with MECA32 in tumor vasculature (**E** and **F**). Original magnifications: 200–400×.

in the various tumor microenvironments, but with one commonality: each homed to the neovasculature in subcutaneous matrigel pellets infused with a mixture of VEGF and bFGF. Neither peptide homed to angiogenic islets (dysplasias) or tumors in the RIP-Tag transgenic mouse model of pancreatic islet cell carcinoma (Hanahan, 1985) (Figures 4A and 4F), indicating that the binding moieties for these peptides are not present in normal, dysplastic, or pancreatic tumor vasculature. Interestingly, both CGKRK and CDTRL did home to breast carcinomas in another transgenic model, the MMTV-PyMT mice (Guy et al., 1992) (Figures 4B and 4G). Some of the positive cells appeared to be circulation-accessible tumor cells (Figure 4G; Chang et al., 2000), and they were negative for the Fcγ-II/III receptors (data not shown), suggesting that the peptide binding moiety can have broader representation beyond tumor endothelial cells. Both the CGKRK and CDTRL bind a range of cultured tumor cells (Supplemental Table S1 online) in addition to homing to tumor endothelial cells in vivo. Further, the activated endothelium in this type of mouse breast tumor shares molecular determinants with SCCs of the skin as detected by these peptides, ones that are not found in the RIP-Tag model of endocrine pancreatic cancer. This commonality is despite the fact that squamous tumorigenesis in the skin was induced by the E6 and E7 oncogenes of HPV16, while the islet tumors in RIP1-Tag2 were induced by the SV40 Tag oncogene, and the mammary tumors in MMTV-PyMT mice were induced by the polyoma middle T antigen.

The two tumor peptides showed different homing to three types of subcutaneously grown transplanted tumors. Fluorescein-CGKRK peptide homed to cells in each of the three transplant tumors (Figures 4C–4E), which arose from PDSC5, a K14-HPV16 tumor-derived cell line (Figure 4C), the MDA-MB-435 human breast cancer line (Figure 4D; Price et al., 1990), and the C8161 human melanoma line (Figure 4E; Bregman and Meyskens, 1986). In contrast, the CDTRL peptide was not present in the PDSC5 (Figure 4H) or MDA-MB-435 (Figure 4I) and only accumulated in the melanoma xenograft (Figure 4J) and in the skin overlying the melanoma xenograft tumor (Figure 4J inset). Fluorescein-CGKRK localized in the cytoplasm and nuclei of vascular cells identified as endothelial cells by their morphology and by immunostaining for CD31 and MECA32 (exemplified by Figure 4D). In addition, the peptide apparently extravasated out of the vessels and became distributed along tendril-like structures and in tumor cell nuclei; it also accumulated to some extent in avascular necrotic regions (exemplified by Figures 4B, 4C, and 4E). Given that all three tumors were growing subcutaneously, presumably by recruiting a neovasculature from the same normal vascular bed in the dermis, one can infer that cell type and/or oncogenic stimulus is imparting different qualities onto the vasculature and the tumor microenvironment, as revealed by the differential homing patterns seen with these peptides. Furthermore, it is apparent that the matrigel extracellular matrix in combination with VEGF and bFGF is sufficient to elicit expression of the binding moieties for these homing peptides;

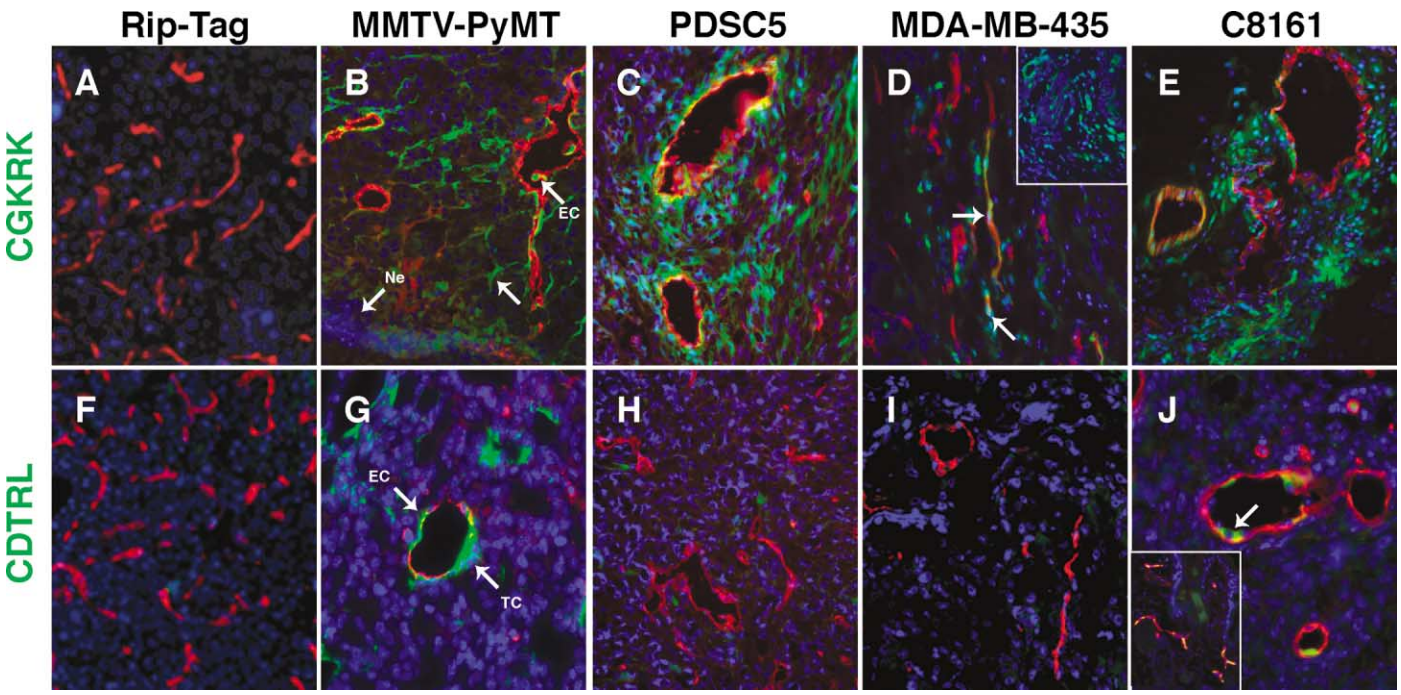

Figure 4. Localization of fluorescein-labeled peptides in other tumors

Mice bearing various tumors were intravenously injected with fluorescein-labeled peptides from the tumor-homing phage and examined as in Figure 3. The tissue sections were stained with MECA32 (shown with red fluorochrome) and CD31 (not shown). Fluorescein-CGKRK (**A–E**) was detected in 4 of the 5 tumor models examined; RIP1-Tag2 tumors (**A**) were negative. Some features are indicated by arrows, with the labels EC (for endothelial cell), TC (for tumor cell), and Ne (for necrotic region). The CGKRK peptide was seen in endothelial cells and tumor cells appearing both in the cytoplasm and nucleus (**B–E;** arrow in **D**). Fluorescein-CDTRL (**F–J**) was absent in the RIP1-Tag2 tumors (**F**), PDSCJ5 (**H**), and MDA-MB-435 (**I**), but present in MMTV-PyMT tumors (**G**) and C8161 xenografts (**J**) tumors. In the C8161 xenografts, the positive cells were CD31-positive cells that were adhering and spreading on the lumenal surface of the blood endothelial cells; the established endothelia were negative (indicated by the white arrow in **J**). The blood vessels in the skin surrounding the C8161 xenograft tumor are also positive for fluorescein-CDTRL (**J** inset). In the MMTV-PyMT, fluorescein-CDTRL colocalized with CD31 and MECA32 and also bound to cells within the vessel wall that were negative for MECA32, CD31, and the Fcγ-II/II receptors (**G**). Original magnifications: 200–400×.

notably, the neovasculature is again recruited from the dermis. Moreover, the two growth factors used in the matrigel assay have been implicated in the angiogenesis associated with squamous carcinogenesis of the skin in the K14-HPV16 model (Arbeit et al., 1996; Coussens et al., 1999).

Discussion

In the study described herein, we have used phage libraries to profile the vascular changes that take place during squamous carcinogenesis of the skin in a transgenic mouse model involving the human papillomavirus type 16 oncogenes, which are implicated as causative agents in human squamous cancers. We describe three peptides that distinguish between the neovasculature in premalignant dysplastic lesions and malignant tumors. The peptides also distinguish both types of vasculature from normal skin vasculature. The in vivo binding patterns also reveal molecular diversity in the vasculature of tumors of different origins and anatomical locations, consistent with predictions based on evident morphological differences (Roberts et al., 1998).

The CSRPRRSEC peptide, obtained by screening for homing to dysplastic skin lesions, clearly differentiated this class of lesions from normal skin and from fully developed skin tumors. Moreover, because the peptide localized to the endothelial cells of the dysplastic lesions, the selectivity of its homing is attributable to vascular changes during the carcinogenic progression from normal skin to dysplasia to cancer. The accompanying paper (Joyce et al., 2003) describes peptides with different sequences that selectively recognize premalignant angiogenic islets in RIP1-Tag2 mice. Thus, the vasculature of premalignant lesions can be distinguished from that of malignant tumors of the same lineage in two different tumor systems.

The tumor-specific peptide CGKRK showed the broadest selectivity, homing to all tumors growing in or under the skin, while the CSRPRRSEC and CDTRL peptides were selective for two of the four tumors tested. The three tumor-selective phage did not home to normal skin vasculature and showed variable selectivity toward dysplasias of tumor-bearing mice. While all three homed to transplant tumors and the VEGF/bFGF matrigels, none accumulated in the angiogenic islet dysplasias or solid tumors in the RIP1-Tag2 model of pancreatic islet carcinogenesis. The strain of mice used did not seem to affect the homing of these peptides, as evidenced by their homing to tumors in different strains and their differential homing to tumors within the same strain. For example, the CGKRK peptide homed to tumors in FVB/b, C57B16, and Balb/c-*nu/nu*, while the CDTRL homed to C8161 but not MDA-MB-435 tumors, each growing in Balb/c-*nu/nu* mice. In the companion manuscript, Joyce et al. (2003) report a panel of peptides that home to the vasculature

of angiogenic islets and pancreatic islet carcinomas but not to the skin dysplasias or tumors in the HPV16 mice, nor to the vasculature in several subcutaneous transplant tumors or in s.c. matrigel plugs. Together, the data demonstrate that tumorigenesis in different organs involves the induction of distinctive vascular signatures as revealed by the selection of peptides displayed on circulating phage.

A database search revealed a homology between our CSRPRRSEC peptide and the C_{220}SRPRR$_{225}$ sequence in human kallikrein-9 (Yousef and Diamandis, 2000) and its mouse homolog (RIKEN Clone 1200016C12; Kawai et al., 2001), both proteases of the trypsin super family. These particular residues appear to be critical for the homing of the CSRPRRSEC peptide, as evidenced by the recovery of the CSRPRRSVC and CSRPRRSWC variants in our selection. The Cys220 to Arg225 sequence of human kallikrein-9 forms a loop that is part of the entrance to the active site; its conformation is variable between the different kallikreins and trypsin family members, affecting substrate specificity (Gomis-Ruth et al., 2002). Our cyclic peptide could structurally resemble and functionally mimic this loop. In the kallikreins, Cys220 forms a disulfide bond with Cys190, the cysteine next to the active site nucleophile Ser195, and all kallikreins close this loop with a kink introduced by the invariant Pro226. Our peptide closes the loop by forming a disulfide bond. Besides the sequence and structural identity, human kallikrein-9 is known to be expressed in the skin (Yousef and Diamandis, 2000), and the protein has been reported to be a favorable prognostic marker in ovarian cancer, implying that it antagonizes ovarian carcinogenesis (Yousef et al., 2001); moreover, several kallikreins are antiangiogenic (Diamandis et al., 2000). Thus, the receptor for the CSRPRRSEC peptide may be a kallikrein-9 substrate or inhibitor that is expressed or localized at elevated levels on the angiogenic endothelia of dysplastic skin lesions but then decreases with progression to squamous carcinomas. In analogy, PSA (prostate-specific antigen or human kallikrein-3) can cleave plasminogen to generate angiostatin (Heidtmann et al., 1999); kallikrein binding proteins like kallistatin are involved in angiogenesis (Miao et al., 2002) and kallikreins can exist as complexes with endogenous inhibitors on the surface of cells (Yayama et al., 2003). The possible functional involvement of this protease and its substrates and inhibitors in the HPV16 model squamous carcinogenesis deserves future investigation.

The CGKRK tumor-homing peptide was found in association with the luminal surface of the tumor endothelium, but also inside the tumor parenchyma after an intravenous injection. The localization of the peptide within the tumor tissues was not simply a result of leakiness of the tumor vasculature to labeled peptides because we did not see the same distribution with the other fluorescein-labeled peptides, and only the CGKRK peptide became localized to the nuclei of the tumor cells.

The CGKRK tumor-homing peptide has an overall charge of +3 and is essentially composed of basic residues. This peptide may bind by virtue of this charge and composition to cell surface heparan sulfates and to phosphatidylserine. An ~60 nm in diameter T7 phage displaying 415 copies of this peptide would resemble a cationic liposome; cationic liposomes bind to and are used as a marker of tumor vasculature (Thurston et al., 1998). Cationic particles may bind to phosphatidylserine, an anionic phospholipid that is on the surface of tumor endothelial cells and is accessible to circulation (Ran et al., 2002). Phosphatidylserine is also a marker of apoptotic cells, and the phosphatidylserine receptor on macrophages mediates engulfment (Fadok et al., 2000); this could explain CGKRK's uptake by the necrotic/apoptotic regions in the tumors (like shown in Figure 4B).

The KRK sequence is also found in exon 6 of human and mouse VEGF-A and other VEGF homologs like the endocrine gland-specific protein Bv8 (LeCouter et al., 2003). Exon 6 is present in the highly basic, cell-associated forms of VEGF ($VEGF_{189}$ and $VEGF_{206}$). Synthetic peptides corresponding to exon 6 release both FGF-2 and VEGF from the cell surface (Jonca et al., 1997) and inhibit VEGF binding and activity on HUVECs (Jia et al., 2001). A 24 residue basic peptide from exon 7 of $VEGF_{165}$ has been expressed on phage and shown to bind to heparan sulfate and home to the vasculature of subcutaneously growing CT26 colon and MATB-III mammary adenocarcinomas (El-Sheikh et al., 2002). The homing of heparin binding peptides to tumor vasculature may be explained by a greater accessibility to heparan sulfates or the expression of other specific glycosaminoglycans. Indeed there are known cases of glycosaminoglycans being preferentially expressed on the blood vessels of tumors (Smetsers et al., 2003; Qiao et al., 2003). The functional importance of this sequence in VEGF-A is suggested by the fact that mice engineered to express only $VEGF_{120}$, which lacks the ability to bind heparin, die within 2 weeks postpartum (Carmeliet et al., 1999). The CGKRK peptide may have a similar specificity, as it recognized the vessels in each of the subcutaneous tumors as well as the neovasculature induced in matrigel pellets implanted with VEGF and bFGF (Supplemental Figure S3 on *Cancer Cell* website).

Basic FGF binds to heparan sulfate and is also internalized by cells in a process that can be distinguished from internalization via FGF receptors (Roghani and Moscatelli, 1992), suggesting that heparan sulfate binding could be responsible for internalization of the CGKRK peptide. Finally, KRK is a known nuclear localization sequence (Craggs and Kellie, 2001; Zhou et al., 1991), potentially explaining the nuclear localization of the CGKRK peptide we observed. SCC induced in the skin by HPV oncogenes could therefore differ from islet cell tumors in the composition or presence of glycosaminoglycans like heparan sulfate, a possibility that deserves future investigation.

A similar shared specificity between tumor endothelial and tumor cells has been previously reported for two other tumor-homing peptides (Laakkonen et al., 2002; Porkka et al., 2002); these reported peptides are also internalized by cells and become localized to the nuclei. Tumor-homing peptides that penetrate into the tumor and are internalized by overt cancer cells or tumor endothelial cells may be particularly well suited for targeting therapeutic and imaging agents into tumors, leveraging their specificity and ability to accumulate substantively therein.

In summary, we describe peptides that target different stages of tumor development in the K14-HPV16 model of squamous cell carcinoma of the skin. These peptides further reveal molecular differences between tumor types. Peptides such as these and the receptor moieties they detect by their selective binding will contribute to our understanding of vascular heterogeneity and temporal changes that occur during multistage tumor development in different organs. This knowledge will provide avenues for developing improved diagnostic tools, including ones affording early detection of premalignant lesions and

asymptomatic early stage carcinomas, as well as for targeting therapeutics to those lesions.

Experimental procedures

Tumor-bearing and transgenic mice

To investigate homing to dysplasias, we used K14-HPV16 mice at 4–6 months of age and with no macroscopic evidence of tumors. Tumor-bearing K14-HPV16 mice were 9–12 months old with obvious ear or trunk tumors. RIP1-Tag2 mice were used at 12 weeks of age, when 100% had pancreatic islet tumors. MMTV-PyMT mice were 4–6 months old, bearing palpable mammary tumors. Cells for subcutaneous inoculation to produce the transplant tumors were cultured in 10% fetal calf serum (FCS) in Dulbecco's Modified Eagle's Media (DMEM). Tumors were generated by subcutaneously injecting 10^6 cells into the chest skin of FVB/n (PDSC5) or Balb/c nude (MDA-MB-435 and C8161) mice. We used mice bearing s.c. transplant tumors with an approximate diameter of 1 cm. PDSC5 tumors and MDA-MB-435 xenografts reached this size about 9 weeks post-injection while C8161 xenografts took 3 weeks post-injection. The matrigel angiogenesis bioassay involved inoculating Balb/c-*nu/nu* mice with a gelatinous plug composed of a mixture of 400 μl of Matrigel (Becton Dickinson, Bedford, Massachusetts), 100 ng of basic fibroblast growth factor, and 50 ng of vascular endothelial growth factor (R&D Systems, Minneapolis, Minnesota) in a 450 μl final volume. There were three experimental groups, one for each of the three peptides, comprised of three mice in each group. The mice were injected i.v. with 100 μg of fluorescein-peptide 9 days post-implantation. All animal experiments were approved by the Animal Research Committees at the Burnham Institute or University of California at San Francisco.

Ex vivo and in vivo phage selections

The selections were made with an NNK-encoded CX_7C peptide library displayed on Novagen's T7 415-1b phage vector. The library had a diversity of approximately 1×10^8. Phage selections and validations have been described (Hoffman et al., 2004; Laakkonen et al., 2002).

Immunofluorescence and immunohistochemistry

Areas of skin, tumors, and various organs were collected and either fixed in formalin, dehydrated through serial alcohols, and embedded in paraffin or directly embedded in OCT medium (Fisher Scientific). The K14-HPV16 dysplasia and tumors were graded by evaluating hematoxylin & eosin and anti-keratin staining on 5 μm paraffin sections under a light microscope (Coussens et al., 1996). Rat anti-mouse CD31, rat anti-mouse MECA32, and anti-CD16/CD32 (FcγRII and FcγRIII; BD Pharmingen) were used for vascular immunostaining on 10 μm frozen sections. The anti-phage stainings and biodistribution of fluorescein-labeled peptides were conducted as previously described (Hoffman et al., 2004; Laakkonen et al., 2002).

Acknowledgments

The authors thank Jeff Nickel and Cherry Concengco for excellent technical assistance with histology and Dr. Fernando Ferrer for peptide syntheses. This work was supported by grant PO1 CA 82713 (E.R. and D.H.), Cancer Center Support Grant CA 30199 (The Burnham Institute), and by other grants from the NIH (D.H.). J.A.H. was supported by NCI training grant T32 CA77109-05, M.S. by a postdoctoral fellowship from the California Cancer Research Program.

Received: June 5, 2003
Revised: September 10, 2003
Published: November 24, 2003

References

Arap, W., Pasqualini, R., and Ruoslahti, E. (1998). Cancer treatment by targeted drug delivery to tumor vasculature in a mouse model. Science *279*, 377–380.

Arbeit, J., Munger, K., Howley, P., and Hanahan, D. (1994). Progressive squamous epithelial neoplasia in K14-human papillomavirus type 16 transgenic mice. J. Virol. *68*, 4358–4368.

Arbeit, J., Olson, D., and Hanahan, D. (1996). Upregulation of fibroblast growth factors and their receptors during multi-stage epidermal carcinogenesis in K14-HPV16 transgenic mice. Oncogene *13*, 1847–1857.

Bergers, G., Javaherian, K., Lo, K., Folkman, J., and Hanahan, D. (1999). Effects of angiogenesis inhibitors on multistage carcinogenesis in mice. Science *284*, 808–812.

Bergers, G., Song, S., Meyer-Morse, N., Bergsland, E., and Hanahan, D. (2003). Benefits of targeting both pericytes and endothelial cells in the tumor vasculature with kinase inhibitors. J. Clin. Invest. *111*, 1287–1295.

Bregman, M., and Meyskens, F.J. (1986). Difluoromethylornithine enhances inhibition of melanoma cell growth in soft agar by dexamethasone, clone A interferon and retinoic acid. Int. J. Cancer *37*, 101–107.

Burg, M., Pasqualini, R., Arap, W., Ruoslahti, E., and Stallcup, W. (1999). NG2 proteoglycan-binding peptides target tumor neovasculature. Cancer Res. *59*, 2869–2874.

Carmeliet, P., and Jain, R. (2000). Angiogenesis in cancer and other diseases. Nature *407*, 249–257.

Carmeliet, P., Ng, Y.S., Nuyens, D., Theilmeier, G., Brusselmans, K., Cornelissen, I., Ehler, E., Kakkar, V.V., Stalmans, I., Mattot, V., et al. (1999). Impaired myocardial angiogenesis and ischemic cardiomyopathy in mice lacking the vascular endothelial growth factor isoforms VEGF164 and VEGF188. Nat. Med. *5*, 495–502.

Chang, Y.S., di Tomaso, E., McDonald, D.M., Jones, R., Jain, R.K., and Munn, L.L. (2000). Mosaic blood vessels in tumors: Frequency of cancer cells in contact with flowing blood. Proc. Natl. Acad. Sci. USA *97*, 14608–14613.

Coussens, L., Hanahan, D., and Arbeit, J. (1996). Genetic predisposition and parameters of malignant progression in K14-HPV16 transgenic mice. Am. J. Pathol. *149*, 1899–1917.

Coussens, L., Raymond, W., Bergers, G., Laig-Webster, M., Behrendtsen, O., Werb, Z., Caughey, G., and Hanahan, D. (1999). Inflammatory mast cells up-regulate angiogenesis during squamous epithelial carcinogenesis. Genes Dev. *13*, 1382–1397.

Coussens, L., Tinkle, C., Hanahan, D., and Werb, Z. (2000). MMP-9 supplied by bone marrow-derived cells contributes to skin carcinogenesis. Cell *103*, 481–490.

Craggs, G., and Kellie, S. (2001). A functional nuclear localization sequence in the C-terminal domain of SHP-1. J. Biol. Chem. *276*, 23719–23725.

Diamandis, E., Yousef, G., Luo, L., Magklara, A., and Obiezu, C. (2000). The new human kallikrein gene family: implications in carcinogenesis. Trends Endocrinol. Metab. *11*, 54–60.

El-Sheikh, A., Liu, C., Huang, H., and Edgington, T.S. (2002). A novel vascular endothelial growth factor heparin-binding domain substructure binds to glycosaminoglycans in vivo and localizes to tumor microvascular endothelium. Cancer Res. *62*, 7118–7123.

Fadok, V., Bratton, D., Rose, D., Pearson, A., Ezekewitz, R., and Henson, P. (2000). A receptor for phosphatidylserine-specific clearance of apoptotic cells. Nature *405*, 85–90.

Gee, M.S., Procopio, W.N., Makonnen, S., Feldman, M.D., Yeilding, N.M., and Lee, W.M.F. (2003). Tumor vessel development and maturation impose limits on the effectiveness of anti-vascular therapy. Am. J. Pathol. *162*, 183–193.

Gomis-Ruth, F.X., Bayes, A., Sotiropoulou, G., Pampalakis, G., Tsetsenis, T., Villegas, V., Aviles, F.X., and Coll, M. (2002). The structure of human prokallikrein 6 reveals a novel activation mechanism for the kallikrein family. J. Biol. Chem. *277*, 27273–27281.

Guy, C., Cardiff, R., and Muller, W. (1992). Induction of mammary tumors by expression of polyomavirus middle T oncogene: a transgenic mouse model for metastatic disease. Mol. Cell. Biol. *12*, 954–961.

Hanahan, D. (1985). Heritable formation of pancreatic beta-cell tumours in transgenic mice expressing recombinant insulin/simian virus 40 oncogenes. Nature *315*, 115–122.

Hanahan, D., and Folkman, J. (1996). Patterns and emerging mechanisms of the angiogenic switch during tumorigenesis. Cell *86*, 353–364.

Hanahan, D., and Weinberg, R. (2000). The hallmarks of cancer. Cell *100*, 57–70.

Heidtmann, H., Nettelbeck, D., Mingels, A., Jager, R., Welker, H., and Kontermann, R. (1999). Generation of angiostatin-like fragments from plasminogen by prostate-specific antigen. Br. J. Cancer *81*, 1269–1273.

Hoffman, J., Laakkonen, P., Porkka, K., Bernasconi, M., and Ruoslahti, E. (2004). In vivo and ex vivo selections using phage-displayed libraries. In Phage Display: A Practical Approach, in press.

Jia, H., Jezequel, S., Lohr, M., Shaikh, S., Davis, D., Soker, S., Selwood, D., and Zachary, I. (2001). Peptides encoded by exon 6 of VEGF inhibit endothelial cell biological responses and angiogenesis induced by VEGF. Biochem. Biophys. Res. Commun. *283*, 164–173.

Jonca, F., Ortega, N., Gleizes, P.-E., Bertr, N., and Plouet, J. (1997). Cell release of bioactive fibroblast growth factor 2 by exon 6-encoded sequence of vascular endothelial growth factor. J. Biol. Chem. *272*, 24203–24209.

Joyce, J.A., Laakonen, Bernasconi, M., Bergers, G., Ruoslahti, E., and Hanahan, D. (2003). Stage-specific vascular markers revealed by phage display in a mouse model of pancreatic islet tumorigenesis. Cancer Cell *4*, this issue, 393–403.

Kawai, J., Shinagawa, A., Shibata, K., Yoshino, M., Itoh, M., Ishii, Y., Arakawa, T., Hara, A., Fukunishi, Y., Konno, H., et al. (2001). Functional annotation of a full-length mouse cDNA collection. Nature *409*, 685–690.

Laakkonen, P., Porkka, K., Hoffman, J., and Ruoslahti, E. (2002). A tumor-homing peptide with a targeting specificity related to lymphatic vessels. Nat. Med. *8*, 751–755.

LeCouter, J., Lin, R., Tejada, M., Frantz, G., Peale, F., Kenneth, J.H., and Ferrara, N. (2003). The endocrine-gland-derived VEGF homologue Bv8 promotes angiogenesis in the testis: Localization of Bv8 receptors to endothelial cells. Proc. Natl. Acad. Sci. USA *100*, 2685–2690.

Miao, R.Q., Agata, J., Chao, L., and Chao, J. (2002). Kallistatin is a new inhibitor of angiogenesis and tumor growth. Blood *100*, 3245–3252.

Pasqualini, R., Arap, W., and McDonald, D. (2002). Probing the structural and molecular diversity of tumor vasculature. Trends Mol. Med. *8*, 563–571.

Porkka, K., Laakkonen, P., Hoffman, J., Bernasconi, M., and Ruoslahti, E. (2002). A fragment of the HMGN2 protein homes to the nuclei of tumor cells and tumor endothelial cells in vivo. Proc. Natl. Acad. Sci. USA *99*, 7444–7449.

Price, J., Polyzos, A., Zhang, R., and Daniels, L. (1990). Tumorigenicity and metastasis of human breast carcinoma cell lines in nude mice. Cancer Res. *50*, 717–721.

Qiao, D., Meyer, K., Mundhenke, C., Drew, S.A., and Friedl, A. (2003). Heparan sulfate proteoglycans as regulators of fibroblast growth factor-2 signaling in brain endothelial cells. Specific role for glypican-1 in glioma angiogenesis. J. Biol. Chem. *278*, 16045–16053.

Ran, S., Downes, A., and Thorpe, P.E. (2002). Increased exposure of anionic phospholipids on the surface of tumor blood vessels. Cancer Res. *62*, 6132–6140.

Roberts, W., Delaat, J., Nagane, M., Huang, S., Cavenee, W., and Palade, G. (1998). Host microvasculature influence on tumor vascular morphology and endothelial gene expression. Am. J. Pathol. *153*, 1239–1248.

Roghani, M., and Moscatelli, D. (1992). Basic fibroblast growth factor is internalized through both receptor-mediated and heparan sulfate-mediated mechanisms. J. Biol. Chem. *267*, 22156–22162.

Ruoslahti, E. (2002). Specialization of tumour vasculature. Nat. Rev. Cancer *2*, 83–90.

Smetsers, T.F., van de Westerlo, E.M., ten Dam, G.B., Clarijs, R., Versteeg, E.M., van Geloof, W.L., Veerkamp, J.H., van Muijen, G.N., and van Kuppevelt, T.H. (2003). Localization and characterization of melanoma-associated glycosaminoglycans: differential expression of chondroitin and heparan sulfate epitopes in melanoma. Cancer Res. *63*, 2965–2970.

Smith-McCune, K., Zhu, Y.H., Hanahan, D., and Arbeit, J. (1997). Cross-species comparison of angiogenesis during the premalignant stages of squamous carcinogenesis in the human cervix and K14-HPV16 transgenic mice. Cancer Res. *57*, 1294–1300.

Thurston, G., McLean, J., Rizen, M., Baluk, P., Haskell, A., Murphy, T., Hanahan, D., and McDonald, D. (1998). Cationic liposomes target angiogenic endothelial cells in tumors and chronic inflammation in mice. J. Clin. Invest. *101*, 1401–1413.

Yayama, K., Kunimatsu, N., Teranishi, Y., Takano, M., and Okamoto, H. (2003). Tissue kallikrein is synthesized and secreted by human vascular endothelial cells. Biochim. Biophys. Acta *1593*, 231–238.

Yousef, G., and Diamandis, E. (2000). The expanded human kallikrein gene family: locus characterization and molecular cloning of a new member, KLK-L3 (KLK9). Genomics *65*, 184–194.

Yousef, G.M., Kyriakopoulou, L.G., Scorilas, A., Fracchioli, S., Ghiringhello, B., Zarghooni, M., Chang, A., Diamandis, M., Giardina, G., Hartwick, W.J., et al. (2001). Quantitative expression of the human kallikrein gene 9 (KLK9) in ovarian cancer: A new independent and favorable prognostic marker. Cancer Res. *61*, 7811–7818.

Zhou, J., Doorbar, J., Sun, X., Crawford, L., McLean, C., and Frazer, I. (1991). Identification of the nuclear localization signal of human papillomavirus type 16 L1 protein. Virology *185*, 625–632.